

The globular cluster NGC 6540*

E. Bica¹, S. Ortolani², and B. Barbuy³

¹ Universidade Federal do Rio Grande do Sul, Dept. de Astronomia CP 15051, Porto Alegre, 91500-970, Brazil

² Università di Padova, Dept. di Astronomia, Vicolo dell'Osservatorio 5, I-35123 Padova, Italy

³ Universidade de São Paulo, IAG, Dept. de Astronomia, CP 9638, São Paulo 01065-970, Brazil

Received June 16, accepted August 10, 1993

Abstract. We have carried out *UBVI* and Gunn *z* CCD photometry and integrated spectroscopy in the range $\lambda\lambda 3700\text{--}10\,000\text{ \AA}$ of NGC 6540, which was previously classified as an open cluster. The observations indicate that we are dealing with a globular cluster of metallicity $[\text{Fe}/\text{H}] \approx -1.0$ with an extended blue horizontal branch but some stars are also present on the red side. We derive a reddening of $E(B - V) = 0.60 \pm 0.10$ and a distance $d = 3.5$ kpc from the Sun. The cluster giant branch is very poorly populated like in some Palomar clusters; however it has a very concentrated nucleus. Bright giants, extended in the E–W direction, are outside the nucleus. Therefore the cluster has many characteristics in common with post core collapse clusters.

A structural analysis by means of stellar isopleths reveals that the cluster is elongated in the N–S direction in the outer parts, whereas the inner contours are progressively twisted towards E–W.

Key words: globular clusters: individual: NGC 6540 – HR diagram

1. Introduction

NGC 6540 ($\alpha_{1950} = 18^{\text{h}}02^{\text{m}}59^{\text{s}}$, $\delta_{1950} = -27^{\circ}46.1$; $l = 3.29^{\circ}$, $b = -3.31^{\circ}$) is classified in compilations as the open cluster OCL11, also designated as Cr364 and ESO456-SC53. Early studies listed in Alter et al. (1970) provide angular sizes from $0.5'$ to $1'$ and rough distance estimates. No Colour Magnitude Diagram (CMD) is available in the literature. An inspection of Sky Survey Schmidt plates reveals a very compact star cluster, unusual for an open cluster, which led us to suspect that it might be a globular cluster. From cross-checking identifications we realized that NGC 6540 is the cluster number 3 in a list of probable globular

clusters by Djorgovski (1987). He suggested that the cluster has a postcollapse core. We also note that his cluster number 2 is catalogued as ESO456-SC38.

In the present study we provide deep CCD images with the ESO 3.55 m NTT and Danish 1.54 m telescopes, as well as CCD integrated spectra in the range $3700\text{--}10\,000\text{ \AA}$ taken with the 1.52 m telescope. Our analysis confirms its nature as a globular cluster.

NGC 6540 is embedded in a rich field only 4.66° from the Galactic center. In Sky Survey plates this field looks like a smaller version of the Baade window, also surrounded by zones of strong absorption. The stellar population and depth of the field are also studied in this paper.

NGC 6540 is very peculiar structurally with a dense elongated nucleus and two clumps of bright stars which extend the cluster in the east-west direction. In Sect. 2 the observations are presented. In Sect. 3 the CMDs are discussed and the basic cluster and field parameters are derived. In Sect. 4 the spectroscopic results are analysed. We study the cluster structure in Sect. 5. The conclusions of this work are summarized in Sect. 6.

2. Observations

2.1. CCD imaging

The observations were carried out in the *UBVRI* Johnson–Cousins and Gunn *z* bands at the Danish 1.54 m telescopes at the European Southern Observatory (ESO), La Silla, Chile in June 1990. We used the 512×320 pixel RCA CCD ESO 5 with pixel size $30\text{ }\mu\text{m}^2$ ($0.47''$ on the sky), with field size $4' \times 2.5'$. We also observed at the NTT with the coated Thomson CCD ESO 17 of pixel size $19\text{ }\mu\text{m}^2$ ($0.15''$), with field size $2.5' \times 2.5'$.

An offset field located at $9'$ north of the cluster was also observed in the same bands as the cluster. The logbook of the observations is given in Table 1. We show in Fig. 1 a Danish *V* frame of the cluster. Notice the compact elliptical nucleus. Some bright stars are located along the E–W direction, giving an extended appearance to the cluster.

Send offprint requests to: S. Ortolani

* Observations collected at the European Southern Observatory, La Silla, Chile

Table 1. Log-book of the observations

Filter	Date	UT	Exp. time (s)	Seeing
<i>Danish-cluster</i>				
V	18.06.90	3 ^h 46 ^m	240	1.2''
V	18.06.90	3 ^h 55 ^m	60	1.3''
B	18.06.90	3 ^h 58 ^m	120	1.1''
B	18.06.90	4 ^h 03 ^m	240	1.0''
R	18.06.90	4 ^h 11 ^m	15	1.0''
I	18.06.90	4 ^h 14 ^m	15	1.0''
z	18.06.90	4 ^h 23 ^m	15	1.1''
z	18.06.90	4 ^h 27 ^m	25	1.1''
z	18.06.90	4 ^h 30 ^m	25	1.1''
U	18.06.90	4 ^h 40 ^m	900	1.5''
B	18.06.90	5 ^h 02 ^m	30	1.5''
<i>Danish-field</i>				
V	18.06.90	5 ^h 13 ^m	30	1.2''
V	18.06.90	5 ^h 17 ^m	600	1.2''
B	18.06.90	5 ^h 32 ^m	1200	1.3''
B	18.06.90	5 ^h 56 ^m	60	1.3''
I	18.06.90	6 ^h 01 ^m	600	1.2''
I	18.06.90	6 ^h 15 ^m	60	1.1''
z	18.06.90	6 ^h 19 ^m	60	1.0''
z	18.06.90	5 ^h 24 ^m	600	1.0''
<i>NTT-cluster</i>				
V	25.05.90	6 ^h 05 ^m	90	1.0''
V	25.05.90	6 ^h 10 ^m	70	1.0''
V	25.05.90	6 ^h 25 ^m	600	1.0''
B	25.05.90	6 ^h 55 ^m	1200	1.25''
B	25.05.90	7 ^h 17 ^m	180	1.25''
B	25.05.90	7 ^h 25 ^m	180	1.25''

The reductions and calibrations were performed at ESO-Garching with the Midas package. The stellar photometry was made with the DAOPHOT code in MIDAS environment. Landolt (1983) standard stars were used for the calibrations. The observing procedures, reductions and photometric errors were discussed in detail in Ortolani et al. (1990, 1992, 1993), where we have analyzed other clusters as well embedded in dense stellar fields.

Due to the crowding conditions the zero point errors of the photometry are around ± 0.02 – 0.03 . The internal photometric errors are in the range 0.04–0.07 mag for $V = 15$ – 17 mag, and 0.07–0.09 between $V = 17$ – 19 . The equivalent errors in $B - V$ are around 0.07 at $V = 16$, up to 0.1 at $V = 18$. While the colour errors grows roughly as expected from independent error combination of the single bands, they are considerably larger than poissonian noise errors. It is also interesting to note that the errors in the less crowded background field are clearly lower, going from 0.03 to 0.06 mag, between $V = 15$ and 19. The linearity deviations, as deduced from the comparison of the 240 and 60 s V exposures are within 2% in the common 4 mag range.

2.2. CCD spectroscopy

The spectroscopic observations were obtained in July 1989 in the near ultraviolet (near UV) and in May 1990 for the visible plus near infrared at the 1.52 m ESO telescope with a Boller & Chivens spectrograph, described as follows:

(a) A front illuminated coated GEC CCD, ESO 14 with 576×385 pixels of size $22 \mu\text{m}^2$ and ESO grating 8 (193 \AA mm^{-1} in first order) with the coverage $\lambda\lambda 3000$ – 5300 \AA , and a slit of $4''$ were used, yielding a spectral resolution of $\Delta\lambda \approx 16 \text{ \AA}$. One exposure of 20 min was taken. The atmospheric cutoff for these near UV spectra occurred at $\lambda \approx 3050 \text{ \AA}$.

(b) A RCA SID 503 high resolution thinned backside illuminated CCD ESO 13 with 1024×640 pixels of size $15 \mu\text{m}^2$ and ESO grating 13 (509 \AA mm^{-1} in first order), covering $\lambda\lambda 3000$ – 10400 \AA , and a slit of $1.5''$, yielding a resolution of $\Delta\lambda \approx 18 \text{ \AA}$. Two exposures of 20 min were taken. The instrumental response provided a useful range in the visible and near infrared ($3700 < \lambda < 9700 \text{ \AA}$) for this configuration.

In all cases, a long slit was set in the E–W direction scanning a total of $40''$ in the N–S direction, centered on the cluster. The slit length projected on the sky is $3.4'$ in (a) and $3.1'$ in (b). This allowed good sky background subtractions.

The standard stars EG 274 and Feige 110 in (a) and EG 274, LTT 3218 and LTT 7987 in (b) were used for the flux calibrations. The reductions were carried out at ESO Garching with the IHAP system. In Sect. 4, we analyse three spatial extractions along the slit: the central $25''$ corresponding to the compact nucleus, the western $33''$ and eastern $15''$ adjacent to the nucleus, where clumps of bright stars are found. We show in Fig. 2 light profiles along the slit for the near UV ($\lambda\lambda 3100$ – 4000 \AA) and the visible plus near infrared ($\lambda\lambda 4500$ – 9500 \AA), where the extracted positions are indicated. A comparison of these profiles shows that the nucleus is bluer than the eastern and western regions. We also extracted a global cluster spectrum encompassing these three regions.

The near UV spectra of configuration (a) were combined to the visible plus near infrared ones of configuration (b), producing the spectra discussed in Sect. 4.

3. The CMD analysis

3.1. CMD morphology

We show in Fig. 3a a V vs. $(B - V)$ CMD of NGC 6540 corresponding to the whole field frame. The most striking features are the cluster brighter sequences: a clear blue Horizontal Branch (HB) at $V \approx 15.9$, $(B - V) \approx 0.45$ and a red clump at $V \approx 14.7$, $(B - V) \approx 1.3$ consisting of a Red Giant Branch (RGB) base and/or a red HB; and the field features: a disk Main Sequence (MS) intercepting the bulge population evolving sequence at $V \approx 18.9$, $(B - V) \approx 0.9$ and the bulge red HB at $V \approx 15.8$, $(B - V) \approx 1.55$.

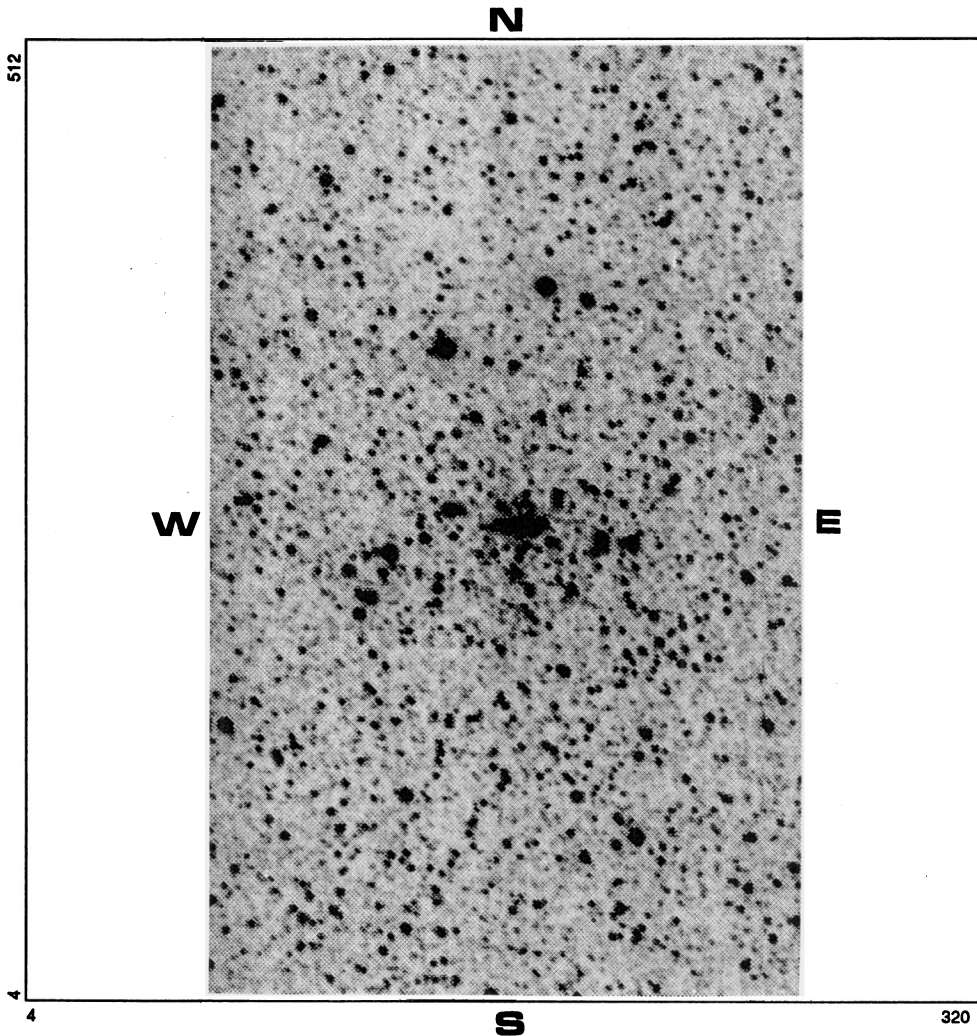


Fig. 1. Danish V frame of NGC 6540 of size $2.5' \times 4.5'$. Axes are in pixels

The cluster sequences are more evident in Fig. 3b, where stars in a circular extraction of $r = 28''$ are plotted over the whole frame field.

Comparing this CMD with those of intermediate metallicity clusters such as NGC 6752 (Aurière & Ortolani 1989), NGC 7006 (Sandage & Wildey 1967) and NGC 288 or M5 (King et al. 1988), NGC 6540 shows a poorly populated giant branch, resembling more to poorly populated Palomar clusters like Pal 13 (Ortolani et al. 1985). On the other hand, it is worth noting that structurally NGC 6540 differs from most Palomar clusters, in the sense that it is very concentrated (see Sect. 5).

Regarding the HB, it has an extended blue one, similar to those of NGC 6752, NGC 288 and M5.

The blue side of the clump of stars at the RGB base contains a few red HB stars. We have estimated the Mironov parameter $B/(B+R)$ taking into account the field background contamination as follows: (i) we defined the blue and red HB zones in the CMDs of NGC 6540 taking the intermediate metallicity clusters as reference; (ii) we counted stars in these zones for a series of cluster circular extractions and for the outer parts of the frame; (iii) from the ana-

lysis of these results we estimate $B/(B+R) = 0.65 \pm 0.15$ for the cluster. This indicates that the cluster CMD morphology resembles more that of M5 rather than that of NGC 288 (with $B/(B+R) = 0.76$ and 0.90 respectively, cf. Zinn 1980).

We have also checked the behaviour of the blue HB in the U vs. $(U-B)$ diagram. The cluster sequences are similar to those seen in Fig. 3b for V vs. $(B-V)$, and we do not find any unusually bright blue HB candidate.

3.2. Spatial CMD analysis

Since the cluster does not have a uniform appearance, we explored in detail the spatial distribution and the nature of the brightest stars.

We show in Fig. 4a, b respectively a very central extraction corresponding to the compact nucleus ($r < 10''$), and a strip of total length $60''$ E-W and total width $20''$ N-S, centered on the nucleus.

The nucleus (Fig. 4a) is dominated by HB and sub-giant branch (SGB) stars, while bright giants are absent. The strip shows well defined cluster sequences, in particular the

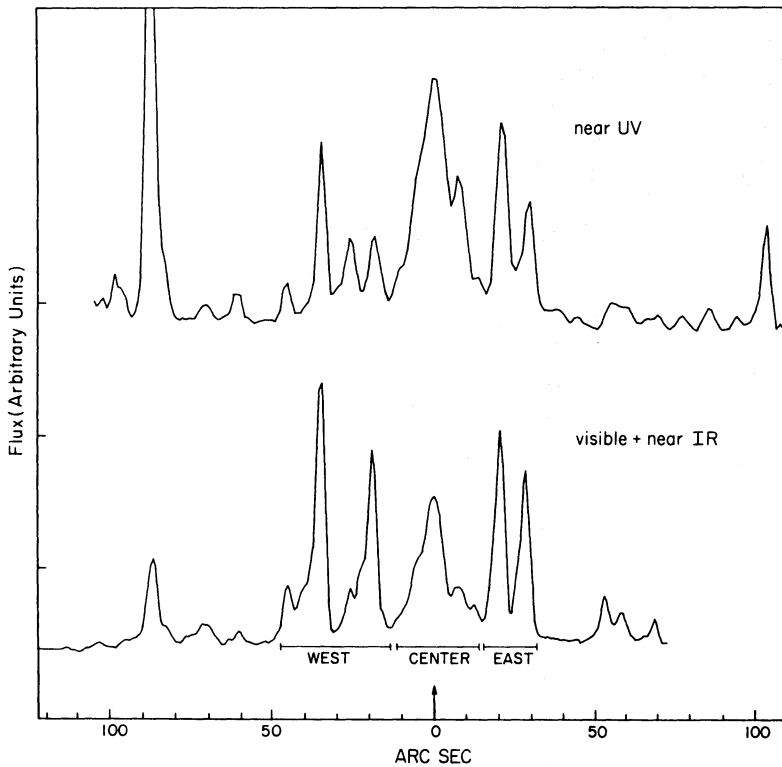


Fig. 2. Light profiles from near UV (upper) and visible plus near IR (lower) spectra. West, center and east positions for spectral extractions are indicated

giant branch appears. Only two bright stars are saturated in the VI frames in the strip, one located to the west and the other to east of the nucleus (Fig. 1), and consequently they do not appear in Fig. 4b. However checking B and R CMDs we verified that they are probably bright tip giants. From this analysis we conclude that bright red giants are dominating the luminosity of the east and west sides, while the nucleus is clearly bluer. This is confirmed by the spectra (Sect. 4).

3.3. Reddening and distance

Using the red edge of the blue HB as reference (NGC 288, NGC 6752, M5 with $(B - V)_0 = 0.15$), and with the observed value of $(B - V) = 0.85$ for NGC 6540, we derive a reddening of $E(B - V) = 0.70 \pm 0.10$.

Taking the mean colour of the red clump $(B - V) = 1.35$ and assuming that it is either a red HB or a RGB at the HB level we made further reddening estimates. With the higher metallicity cluster 47 Tuc (Hesser et al. 1987) we get respectively $E(B - V) = 0.55$ and 0.35 , whereas with a more metal poor one like NGC 7006 we obtain $E(B - V) = 0.85$ and 0.60 . The average value is $E(B - V) = 0.59 \pm 0.11$.

The cluster distance derived from an observed HB level of $V = 15.1$ and a reddening of $E(B - V) = 0.60$ (which fits well also the spectroscopic analysis in Sect. 4) is 3.5 ± 0.4 kpc from the Sun, corresponding to a true distance modulus of $(m - M_0) = 12.7 \pm 0.2$.

Adopting a distance for the Galactic center of 8.0 kpc (Feast 1987) we derive galactocentric coordinates $X \approx 4.5$ kpc, $Y \approx 0.2$ kpc and $Z \approx -0.2$ kpc. Thus the cluster is located very near the Galactic plane, projected close to the Galactic center, nearly halfway between the Sun and the center. In fact, the bulge metal rich field population is strong and the young disk main sequence is relevant in the CMDs throughout this paper.

3.4. Offset field background

As seen in Fig. 3, the background contamination in the cluster frame is important and can be better studied in the offset field V vs. $(B - V)$ shown in Fig. 5. We note the absence of the RGB/red HB and blue HB which characterize the cluster in Fig. 3. Otherwise the features are similar to those seen in the bulge and disk populations of Fig. 3. The center of the red HB is located at $V \approx 17.3$, $(B - V) \approx 1.70$. Comparing these values to those derived from Fig. 3 for the background field in the cluster frame, we conclude that the offset field is in a more reddened region by $\Delta E(B - V) \approx 0.15$ and $\Delta V \approx 0.5$. We also note that the metal-rich giant branch of the bulge population as well as its red HB are considerably wide, indicating distance depth and/or differential reddening.

Taking as reference the Baade Window field (Terndrup 1988), an associated $E(B - V) = 0.5$, and a metal-rich HB level of $M_{V_0} = 1.06$ (Buonanno et al. 1989), we deduce that the bulk of the bulge population in the offset field frame has $E(B - V) \approx 0.63$, and true distance modulus

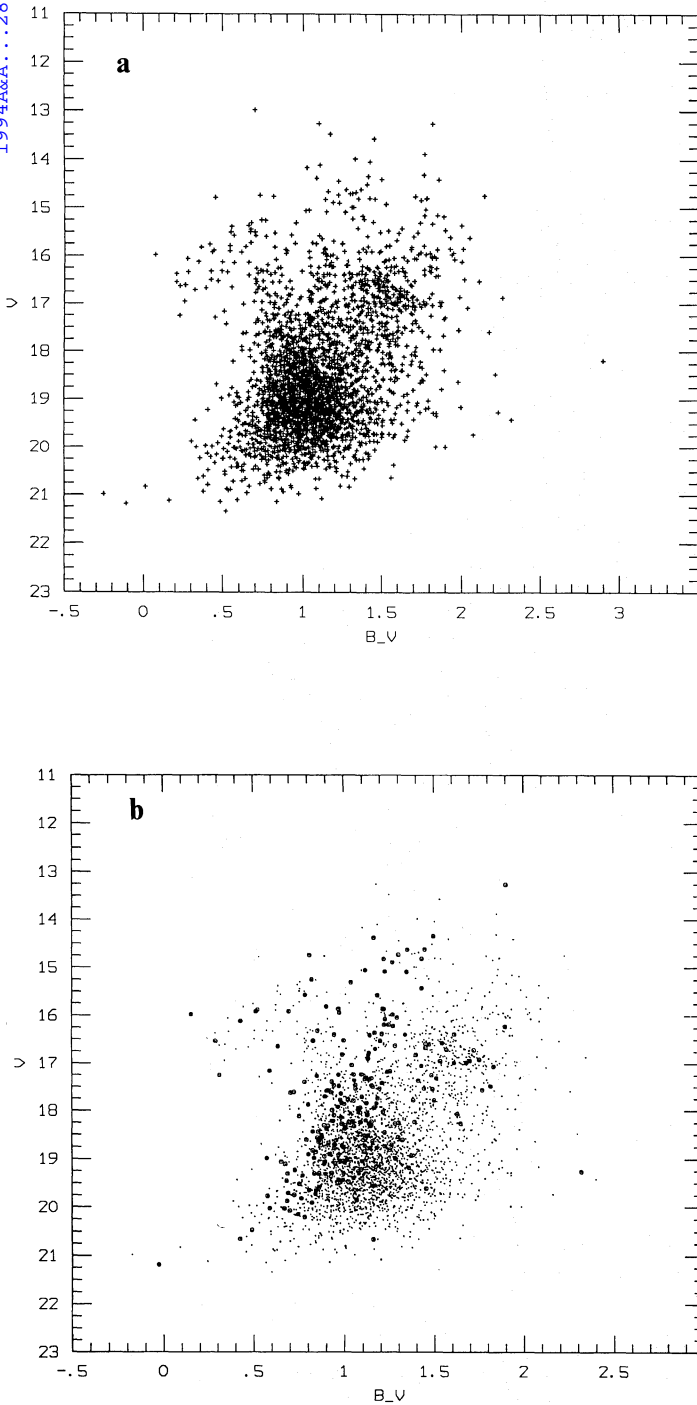


Fig. 3. (a) V vs. $(B - V)$ CMD cluster whole frame from Danish images; (b) same as (a) with stars within $r < 30''$ marked with a circle

$(m - M)_0 = 14.35$, and an average distance of 7.4 kpc. This value increases to 8.4 kpc if $E(B - V) = 0.4$ is assumed for the Baade Window.

We show in Fig. 6 the offset field in V vs. $(V - I)$. The curvature of the giant branch tip is very similar to that of NGC 6528 (Ortolani et al. 1992), indicating that this bulge population is comparable in metallicity to this cluster, which

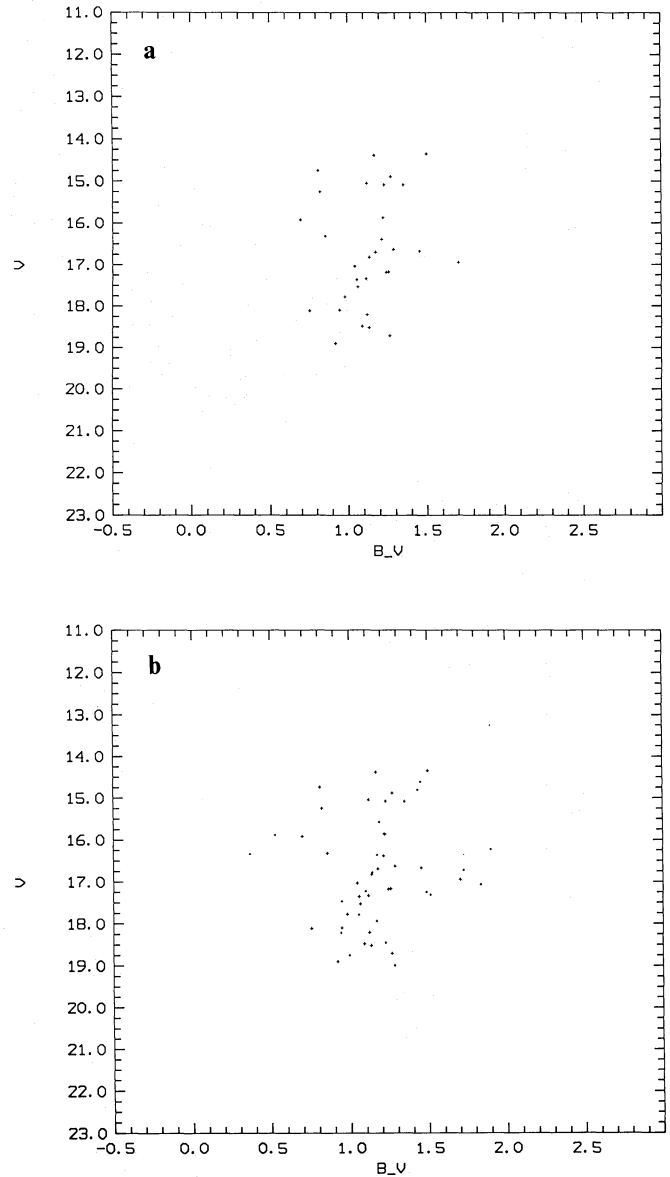


Fig. 4. Cluster V vs. $(B - V)$ CMDs for spatial extractions: (a) stars within $r < 10''$; (b) stars within strip $60''$ (E-W) \times $20''$ (N-S) centered on the cluster

in turn is very similar to that of the Baade Window. This piece of evidence indicates that the bulge population has similar characteristics at this intermediate direction between the minor and major axes, at an angular distance of 4.7° from the Galactic center. On the other hand, the RGB curvature for Terzan 1 and its bulge field (Ortolani et al. 1993) suggests higher metallicity for such more central regions.

4. Spectroscopy

We show in Fig. 7 the observed spectra for the slit extractions of Sect. 2.2. All spectra are normalized to $F_\lambda = 1$ at $\lambda 5870 \text{ \AA}$; the flux ratio of the western and eastern parts relative to the central one are respectively 0.69

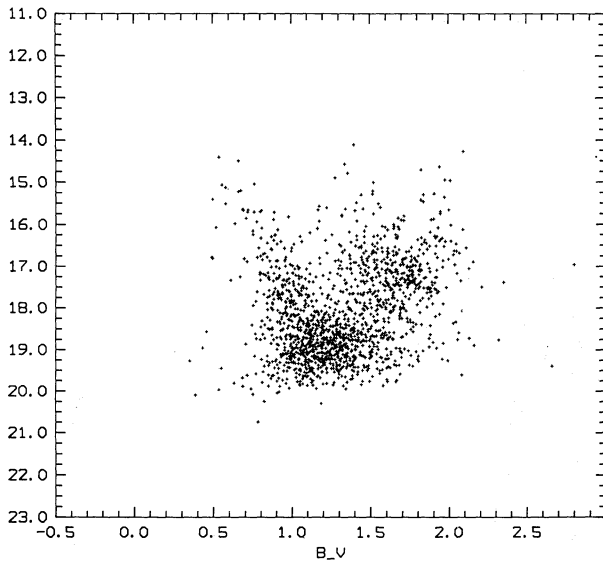


Fig. 5. Offset field V vs. $(B - V)$ CMD

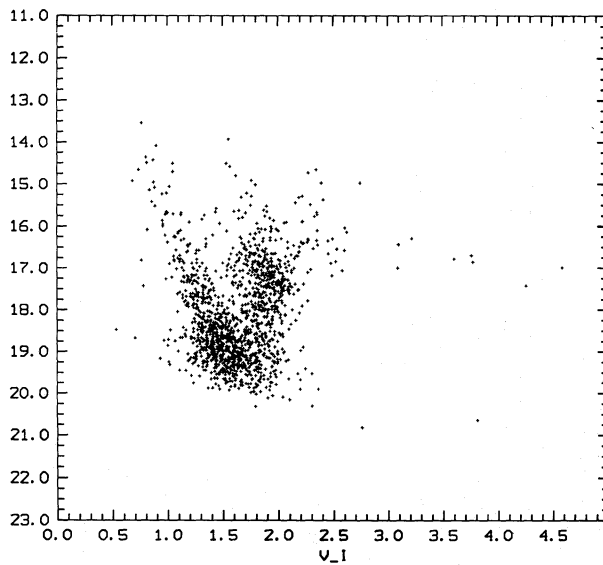


Fig. 6. Offset field V vs. $(V - I)$ CMD

and 1.24 at $\lambda 5870 \text{ \AA}$. The east and west regions are similar and redder than the center, in agreement with the colour analysis of the CMD (Sect. 3.2). Notice the strong Na I absorption occurring in all spectra which is mostly of interstellar origin (see below), suggesting that the stars in the spatial extractions share the same interstellar gas column density.

Following spectral windows and continuum tracings defined in Bica & Alloin (1986a, hereafter BA), we measured equivalent widths (W) for the strongest metallic features and Balmer lines, which are shown in Table 2. Comparing these values with the grid of star clusters as a function of age and metallicity (BA86b), we conclude that the central extraction fits a globular cluster of $[\text{Fe}/\text{H}] \approx -1.0$. On one hand, the central part has no bright giants (Fig. 4a), therefore the metallic features are diluted by the hotter stars; on the other hand, it may be contaminated by bulge metal-rich stars. A compromise value of $[\text{Fe}/\text{H}] \approx -1.0$ seems a reasonable result.

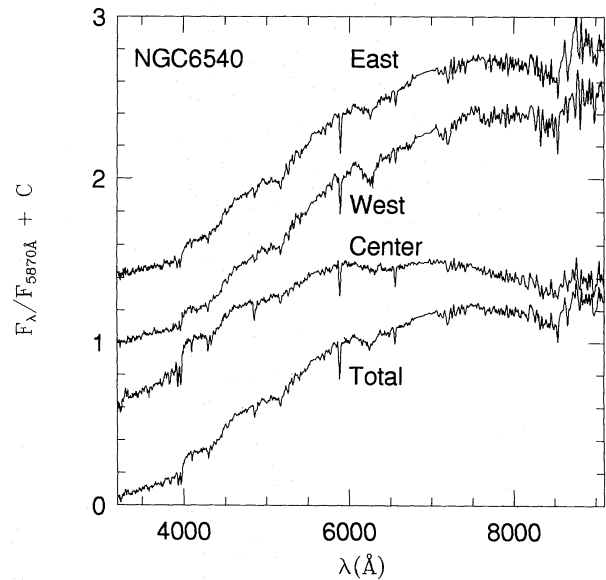


Fig. 7. Cluster observed spectra from extractions along the slit. Flux is in F_λ units, normalized at 5870 \AA

Table 2. Equivalent widths (\AA) in windows defined in BA86a for spatial extractions described in Sect. 2.2

Feature	Window (\AA)	W (Total)	W (Nucleus)	W (West)	W (East)
Ca II K	3908–3952	13.7	11.6	17.4	18.2
Ca II H	3952–3988	12.1	11.1	13.9	14.7
H δ	4082–4124	2.7	2.6	2.4	2.7
CN	4150–4214	5.1	2.2	11.7	6.6
G–CH	4284–4318	7.4	6.1	9.7	8.2
H γ	4318–4364	6.9	6.5	7.6	7.3
H β	4846–4884	3.3	4.2	2.9	3.3
Mg I+Mg H	5156–5196	5.4	3.4	6.6	6.7
Na I	5880–5914	4.6	4.0	5.0	4.9
TiO	6156–6386	11.8	5.2	19.4	12.6

The total spectrum including the E and W extensions, fits rather a higher metallicity ($[\text{Fe}/\text{H}] \approx -0.7$), similar to that 47 Tuc. Two effects may produce stronger features, relative to the central part: the presence of tip cool red giants (Sect. 3.2), and a more pronounced field contamination.

The metallicity value of $[\text{Fe}/\text{H}] \approx -1.0$ seems to be high for a cluster containing a blue extended HB (Zinn 1980). However we note that a blue HB is a characteristic of central regions of core collapsed clusters (Fusi Pecci et al. 1993), which together with the fact that NGC 6540 also contains some stars on the red side (Sect. 3.1) suggests that the enhancement on the blue side might be related to the cluster compact structure.

The large equivalent width of Na I feature (Table 2) is the sum of the stellar component and the interstellar one. The intrinsic value for a cluster of $[\text{Fe}/\text{H}] \approx -1.0$ is $W \approx 1.4 \text{ \AA}$ (BA86b). The interstellar excess is thus $\Delta W(\text{Na I}) \approx 2.9 \text{ \AA}$. According to Fig. 3 of BA86c, this value is consistent with $E(B - V) \approx 0.60$, as derived in Sect. 3.3.

Adopting a reddening value of $E(B - V) = 0.60$ and a normal reddening law, the spectra were dereddened, and the resulting ones for the east, west, center and total extractions are shown in Fig. 8a, b. The east and west parts resemble late type giants as expected, and the central one is that of a globular cluster deficient in red giants, as can be verified in Fig. 8b where populous globular cluster templates of $[\text{Fe}/\text{H}] \approx -1.0$ (G3) and -0.5 (G2) are plotted (Bica 1988). The near UV part of the template spectra are from Bica et al. (1993). Figure 8b shows that the total spectrum of NGC 6540 is also deficient in red light.

Another remark about the spectra concerns the Balmer lines: their presence in Fig. 8, also indicated in Table 2, confirms the occurrence of a blue HB in NGC 6540.

5. Structural properties

An NTT V image (Fig. 9a) indicates that we are dealing with a very concentrated cluster, typical of candidate for post core collapse (Djorgovski & King 1986). An E–W profile extraction through the nucleus indicates a cluster core of $\text{FWHM} \approx 10''$ in the B image; the same value is also obtained from the spectroscopic profiles in Fig. 2. We find for NGC 6540 effects detected in post core collapse clusters (Fusi Pecci et al. 1993) namely a colour gradient with a bluer nucleus, a demise of giants in the center, and an extended blue HB.

We also carried out a surface stellar density analysis. In order to eliminate the bias caused by the few superimposed bright stars on the structure, we have applied the following procedure:

(i) Daophot in Midas environment was used to extract all measurable stars, (ii) the magnitude table was replaced by a single value, (iii) number density contours were created. The results are shown in Fig. 9b. The luminosity excess in the E–W direction disappears, and it is revealed that the outer contours of the globular cluster are elongated

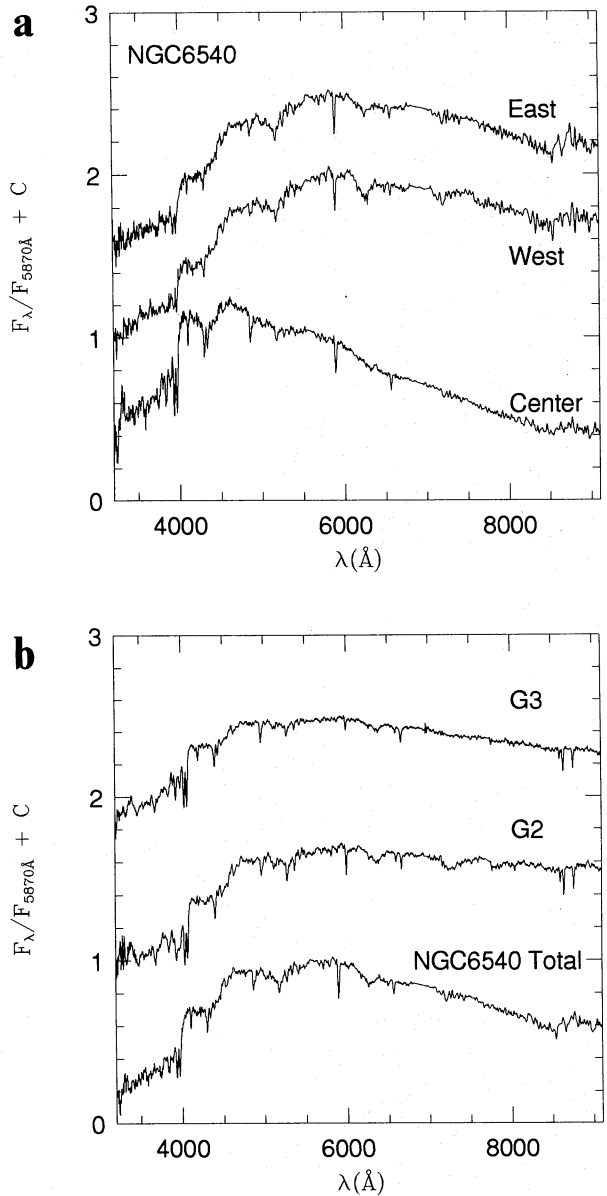


Fig. 8. Reddening corrected spectra: (a) East, west and central extractions; (b) Total extraction and template spectra for globular clusters at $[\text{Fe}/\text{H}] \approx -1.0$ (G3) and ≈ -0.5 (G2)

in the N–S direction. The outer contour indicates a cluster size of approximately $65'' \times 95''$. Furthermore there appears to be a progressive contour twisting for the innermost regions, retrieving the nuclear elongated structure orientation, already visible in the original frame.

The cluster elongation in the V image might be due to an intrinsic structural property and/or distortions caused by irregular dust distribution, since the reddening is high and differential reddening appears to be important in the area (Sects. 3.3 and 3.4). A comparison of cluster images in the near ultraviolet and near infrared (respectively the U and Gunn z frames) sheds light on this question. The U image reveals a patchy dust distribution with a gradient in the N–S direction (the absorption decreases southwards). In the

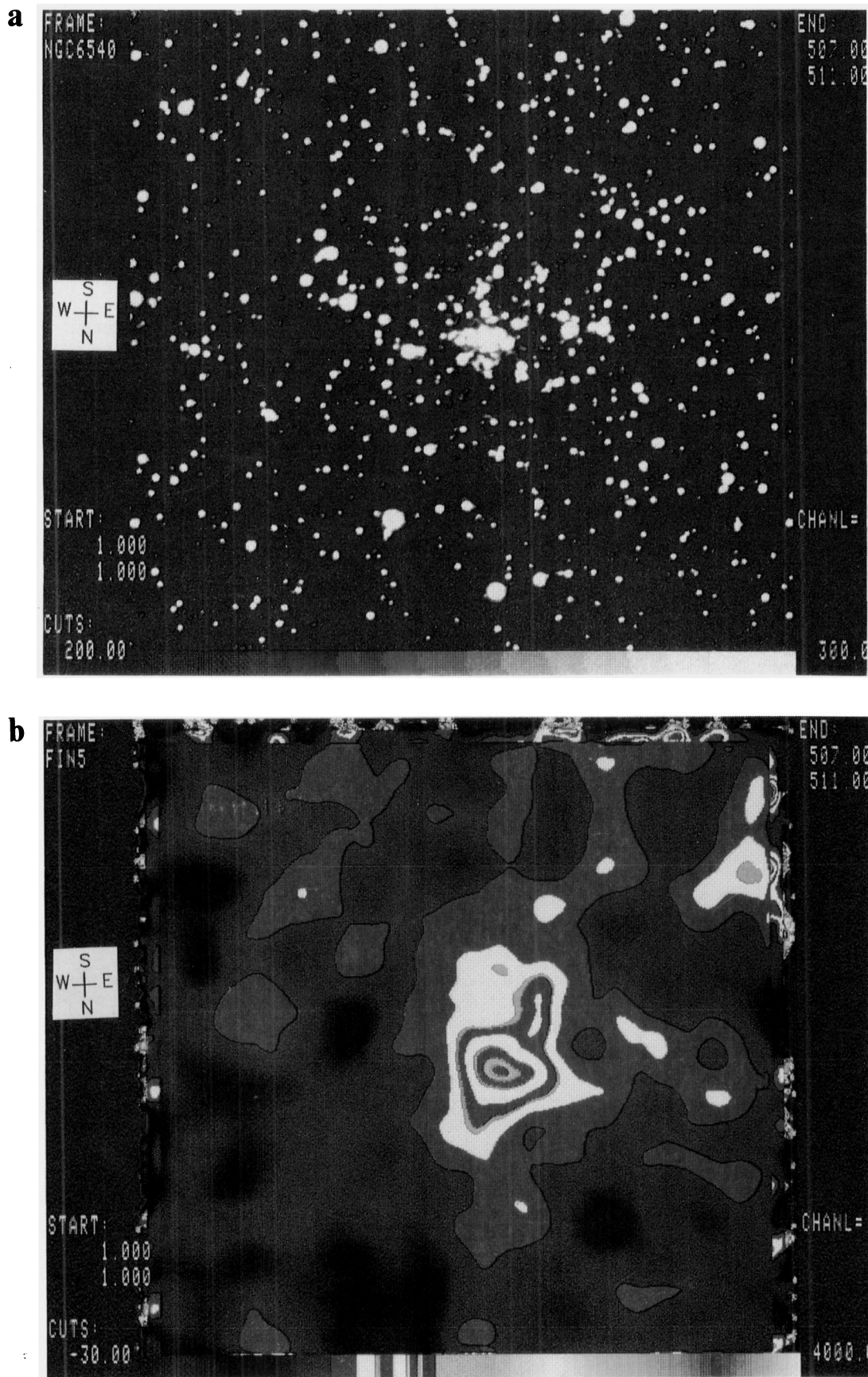


Fig. 9. (a) NTT V image with dimensions $2.5' \times 2.5'$; (b) same as (a) treated for isopleths (Sect. 5)

z image the cluster distribution is much smoother because of the reduced absorption effects. Nevertheless the cluster N–S elongation in the V frame persists in the z one, suggesting that it is intrinsic to the cluster structure. The twisting effect appears to be present also in z .

6. Conclusions

NGC 6540 is not an open cluster as previously catalogued. It is a globular cluster of $[\text{Fe}/\text{H}] \approx -1.0$ with an extended blue horizontal branch, but contains some red horizontal branch stars as well. The cluster is projected on a dense stellar field 4.7° from the Galactic center, with properties similar to those of the Baade Window.

The cluster reddening is $E(B - V) \approx 0.60$ and the distance from the Sun is $d \approx 3.5$ kpc.

The nucleus has $\text{FWHM} = 10''$, and stellar isopleths show that the cluster outer parts are elongated in the N–S direction, and progressively twisting inwards. These effects appear to be intrinsic to the cluster structure rather than being caused by differential reddening.

Some characteristics of this cluster, such as the deficiency of red giants in the center, an extended blue horizontal branch, and the concentrated nucleus, are in common with post collapse clusters.

The cluster complex appearance at first glance might suggest a superposition of an open cluster and a globular cluster, but no compelling evidence for this was found in the CMD analysis. On the other hand, the possibility of a merger of two old clusters cannot be ruled out, owing to the distortion effects on the isopleths.

Acknowledgement. We are grateful to M. Aurière for interesting remarks.

References

- Alter G., Ruprecht J., Vanysek V., 1970, in: Alter G., Balasz B., Ruprecht J. (eds.) *Catalogue of Star Clusters and Associations*, 2nd edn., Akademiai Kiado, Budapest
- Aurière M., Ortolani S., 1989, *A&A* 221, 20
- Bica E., 1988, *A&A* 195, 76
- Bica E., Alloin D., 1986a, *A&A* 162, 21
- Bica E., Alloin D., 1986b, *A&AS* 66, 171
- Bica E., Alloin D., 1986c, *A&A* 166, 83
- Bica E., Alloin D., Schmitt H., 1993 (in preparation)
- Buonanno R., Corsi C.E., Fusi Pecci F., 1989, *A&A* 216, 80
- Djorgovski S., 1987, *ApJ* 317, L13
- Djorgovski S., King I., 1986, *ApJ* 305, L61
- Feast M., 1987, in: Gilmore G., Carswell B. (eds.) *The Galaxy*, NATO ASI series. Reidel, Dordrecht, p. 1
- Fusi Pecci F., Ferraro F.R., Bellazzini M., Djorgovski S., Piotto G., Buonanno R., 1993, *AJ* 105, 1145
- Hesser J., Harris W., Vandenberg D.A., Allwright J.W.B., Shott P., Stetson P., 1987, *PASP* 99, 739
- King C., Demarque P., Green E., 1988, in: Philip A.G.D. (ed.) *Calibration of Stellar Ages*. L. Davis Press, p. 211
- Ortolani S., Barbuy B., Bica E., 1990, *A&A* 236, 362
- Ortolani S., Bica E., Barbuy B., 1992, *A&AS* 92, 441
- Ortolani S., Bica E., Barbuy B., 1993, *A&A* 267, 66
- Ortolani S., Rosino L., Sandage A., 1985, *AJ* 90, 473
- Sandage A., Wildey R., 1967, *ApJ* 150, 469
- Terndrup D.M., 1988, *AJ* 96, 884
- Zinn R., 1980, *ApJ* 241, 602